

Shear strengthening of reinforced concrete beams with CFRP

I. A. Bukhari*, R. L. Vollum†, S. Ahmad* and J. Sagaseta†

Engineering University, Taxila; Imperial College London

The current paper reviews existing design guidelines for strengthening beams in shear with carbon fibre reinforced polymer (CFRP) sheets and proposes a modification to Concrete Society Technical Report TR55. It goes on to present the results of an experimental programme which evaluated the contribution of CFRP sheets towards the shear strength of continuous reinforced concrete (RC) beams. A total of seven, two-span concrete continuous beams with rectangular cross-sections were tested. The control beam was not strengthened, and the remaining six were strengthened with different arrangements of CFRP sheets. The experimental results show that the shear strength of the beams was significantly increased by the CFRP sheet and that it is beneficial to orientate the FRP at 45° to the axis of the beam. The shear strength of FRP strengthened beams is usually calculated by adding individual components of shear resistance from the concrete, steel stirrups and FRP. The superposition method of design is replaced in Eurocode 2 by the variable angle truss model in which all the shear is assumed to be resisted by the truss mechanism. The current paper proposes a methodology for strengthening beams with FRP that is consistent with Eurocode 2.

Introduction

Fibre reinforced polymer (FRP) composites are widely used for strengthening concrete structures because they have many advantages over conventional strengthening methods. Much research has been carried out over the past decade into the performance of concrete beams strengthened in shear with externally bonded FRP composites. Previous experimental studies have shown FRP composites are effective in increasing the shear capacity of reinforced concrete (RC) beams. Despite numerous interesting studies, the shear behaviour of RC beams strengthened with FRP is not well understood. The majority of tests have been carried out on simply supported beams without steel stirrups strengthened with complete side wrap, U-wrap or full wrapping of the section with carbon fibre reinforced polymer (CFRP) sheet. More tests are required to determine whether the increment in shear strength due to CFRP is sensibly independent of the presence

of conventional shear reinforcement as commonly assumed.

Review of current design methods for FRP strengthening in shear

Current American Concrete Institute (ACI 2002 and International Federation for Concrete 2001) design guidelines for strengthening RC beams in shear with CFRP are based on empirical design equations derived by Khalifa *et al.* (1998) and Triantafillou and Antonopoulos (2000) respectively. The nominal shear strength ' V_n ' is calculated by adding individual contributions calculated for the concrete ' V_c ', internal steel stirrups ' V_s ', and external FRP composites ' V_f ' resulting in the general equation

$$V_n = V_c + V_s + V_f \quad (1)$$

where V_c is the shear strength of a beam without stirrups and V_s is calculated with a 45° truss.

The shear contribution of externally bonded FRP reinforcement is calculated analogously to that of internal steel stirrups. Triantafillou (1998) proposed that the contribution of the FRP sheet to shear strength of a RC beam V_f is given by

$$V_f = \rho_f E_f \varepsilon_{fe} b_w z_f (1 + \cot \beta) \sin \beta \quad (2)$$

where b_w is the beam width and E_f is the elastic

65

* Engineering University, Taxila, Pakistan

† Department of Civil and Environmental Engineering, Imperial College London, London, UK

(MACR 800164) Paper received 17 November 2008; last revised 22 January 2009; accepted 11 March 2009

modulus of the FRP. The angle β describes the fibre orientation with respect to the longitudinal axis of the beam. The lever z_f is taken as $0.9 d_f$ in Eurocode format or d_f in ACI (2002) format where d_f is the effective depth of FRP reinforcement measured from the centre of the tensile steel. In the current paper, d_f is measured to the extreme compressive fibre of the FRP when the FRP does not extend over the full height of the beam. The FRP shear reinforcement ratio ρ_f equals $2t_f w_f/(b_w s_f)$ where t_f is the sheet thickness, w_f is the sheet width and s_f is the spacing of the FRP strips which equals w_f for continuous sheets of vertically oriented FRP.

FRP fails at a lower strain than in its naked state when bonded to concrete owing to either de-bonding or rupture. Consequently, the design stress is calculated in FRP in terms of an effective strain (ε_{fe}) which is given by

$$\varepsilon_{fe} = R\varepsilon_{fu} \quad (3)$$

where R is a reduction factor and ε_{fu} is the ultimate tensile strain of FRP.

Calculation of effective stress in FRP

Triantafillou (1998) rearranged Equation 2 to give the effective strain (ε_{fe}) in the FRP in terms of V_f . He found that the effective strain (ε_{fe}) is a function of the axial rigidity ($\rho_f E_f$) of FRP. He went on to derive an empirical relationship between strain and axial rigidity with data from 40 beams tested by various researchers. Khalifa et al. (1998) modified Triantafillou's (1998) method for calculating ε_{fe} on the basis of a slightly enlarged data base of 48 beams. The experimental data used by Khalifa et al. (1998) included two types of FRP materials (carbon and aramid) and three different wrapping configurations (sides only, U-shaped wrapping and complete wrapping), with both continuous sheets and strips of FRP. Khalifa et al. (1998) derived Equation 4a below from a regression analysis of test data including both FRP rupture and de-bonding failure modes. They went on to use Equation 4a to define the effective strain in the FRP at rupture.

$$R = 0.5622(\rho_f E_f)^2 - 1.2188(\rho_f E_f) + 0.778 \quad (4a)$$

for $E_f \rho_f \leq 1.1$ GPa

They defined the reduction factor for CFRP de-bonding (only applicable to side and U wrap) as

$$R = \frac{0.0042(f'_c)^{2/3} w_{fe}}{(t_f E_f)^{0.58} \varepsilon_{fu} d_f} \quad (4b)$$

where w_{fe} is the effective width of the CFRP sheet which is taken as

$$w_{fe} = d_f - nL_e \quad (5)$$

where $n = 1$ for U wrap and 2 for side wrap. Khalifa et al. (1998) took the effective bond length L_e as

$$L_e = e^{[6.134 - 0.58 \ln(t_f E_f)]} \quad (6)$$

Khalifa et al. (1998) took R as the least of 0.5 (to control the shear crack width and loss of aggregate interlock), Equation 4a and Equation 4b if applicable. The lever arm z_f in Equation 2 was taken as d_f . They proposed that the design shear strength should be obtained by multiplying each component of the nominal shear strength by strength reduction factors equal to 0.85 for V_c and V_s and 0.70 for V_f .

Triantafillou and Antonopoulos (2000) presented equations for ε_{fke} which were derived from a regression analysis of data from 75 beam tests. The characteristic effective strain ($\varepsilon_{fke} = 0.8\varepsilon_{fe}$) for fully wrapped CFRP sheet (where shear failure is combined with or followed by FRP rupture) is given by

$$\varepsilon_{fke} = 0.8 \times 0.17 \left(f_c^{2/3} / \rho_f E_f \right)^{0.30} \varepsilon_{fu} \quad (7)$$

and for U-shaped or side wrapped CFRP (where premature shear failure occurs due to de-bonding) is

$$\varepsilon_{fke} = \min \left[0.8 \times 0.65 \left(f_c^{2/3} / \rho_f E_f \right)^{0.56} \times 10^{-3}; 0.8 \times 0.17 \left(f_c^{2/3} / \rho_f E_f \right)^{0.30} \varepsilon_{fu} \right] \quad (8)$$

Equations 7 and 8 should be used with E_f in MPa and $z_f = 0.9d_f$ in Equation 2. Equation 7 was derived from a regression analysis of shear failures combined with or followed by FRP fracture. The first term in Equation 8 was derived from a regression analysis of shear failures combined with FRP de-bonding. Triantafillou and Antonopoulos (2000) proposed that in Eurocode format ε_{fke} should be used in Equation 2 in conjunction with a partial factor of safety of 1.3 if FRP de-bonding governs (i.e. for side or U wraps) or 1.2 if fracture governs (i.e. fully wrapped).

In 2004, The Concrete Society published revised guidelines for strengthening beams in shear with FRP in the second edition of Technical Report (TR) 55 (Concrete Society, 2003). The revised guidelines are based on the work of Denton et al. (2004) and supersede the original recommendations in TR55, which were derived from the work of Khalifa et al. (1998). The contribution of the FRP to the shear capacity is calculated in TR55 (Concrete Society, 2003) with Equation 2 with an effective value for ρ_f given by

$$\rho_f^* = \rho_f (d_f - n l_{tmax} / 3) / z_f \quad (9)$$

where $n = 0$ for fully wrapped sections, 1 for U wrap and 2 for side wrap and l_{tmax} is the anchorage length required to develop full anchorage capacity which is taken as

$$l_{tmax} = 0.7 \sqrt{(E_{td} t_f / f_{ct})} \quad (10)$$

where f_{ct} = tensile strength of concrete = $0.21 f_{ck}^{(2/3)}$

The effective strain in the FRP is taken as the least of (a) $\varepsilon_{fu}/2$, (b) $0.64\sqrt{f_{ct}/E_{fd}t_f}$, (c) 0.004.

According to TR55, the first strain limit represents the average FRP strain when fracture occurs. The second strain limit corresponds to debonding of FRP and the third limit is based on experience and is intended to limit the loss of aggregate interlock due to excessive crack widths. The design stress in the FRP is obtained by multiplying the effective strain by the design elastic modulus which equals the characteristic value divided by a partial factor of safety, which depends on the FRP type and method of application, and which is typically around 1.2.

Zhang and Hsu (2005) presented two equations for calculating R , the least of which is used in Equation 3. They concluded that the fracture of FRP laminates was far more complicated than expected and that there was no simple relationship between R and axial rigidity for FRP fracture. They derived Equation 11 below for bond failure from a regression analysis of beams which failed due to FRP de-bonding:

$$R = 1.4871(\rho_f E_f / f_c)^{-0.7488} \quad (11)$$

Zhang and Hsu (2005) also derived an analytical equation for R from an analysis of bond failure which is similar in principle to that of Khalifa *et al.* (1998).

Assessment and development of existing design recommendations

The present authors assessed the accuracy of the design methods of Khalifa *et al.* (1998), Triantafillou and Antonopoulos (2000) and TR55 (Concrete Society, 2003) by comparing measured and predicted values of V_f (with partial factors of safety equal to 1) for a database of 97 beams strengthened in shear with CFRP. The authors' database includes beams strengthened with side wrapping, U-shaped wrapping and complete wrapping. The data for the beams with side and U wrap are given in Table 1. V_{ftest}/V_{fpred} is plotted against the normalised axial rigidity of the CFRP in Figures 1(a) to 1(c), which show considerable scatter in the accuracy of the predictions of Khalifa *et al.* (1998), Triantafillou and Antonopoulos (2000) and TR55 (Concrete Society, 2003). Triantafillou's (1998) method gives comparatively low values of V_{ftest}/V_{fpred} for side-wrapped specimens as Equation 8 does not distinguish between side and U wrap.

The design method in TR55 (Concrete Society, 2003) differs from the methods of Khalifa *et al.* (1998) and Triantafillou (1998) in that it does not relate the strength reduction factor R to the axial rigidity of the FRP. The present authors carried out a regression analysis to determine whether a statistically significant relationship exists between the effective strain and the axial rigidity of the FRP for the beams in their database. The test data were separated into two categories pertaining to rupture and de-bonding of FRP. The axial

rigidity of the CFRP $\rho_f E_f$ was normalised by $f_c'^{2/3}$ as Horiguchi and Saeki (1997) showed that the bond strength between the concrete and FRP depends on $f_c'^{2/3}$. Best-fit curves are plotted between the effective strain defined in Equation 2 and the normalised axial rigidity $\rho_f E_f / f_c'^{2/3}$ of the FRP in Figures 2(a) and (b). The data points in Figure 2(a) which correspond to rupture of FRP are very scattered indicating that a simple equation based on regression analysis does not capture the complexity of the data. Figure 2(a) also shows the effective strains corresponding to the equations of Khalifa *et al.* (1998) (for $\varepsilon_{fu} = 0.014$) and Triantafillou and Antonopoulos (2000) for FRP fracture. There seems little justification for these equations and it seems sufficient to limit ε_{fe} to $0.4\varepsilon_{fu}$ to avoid CFRP fracture. Separate regression analyses are shown in Figure 2(b) for (a) side wrap and (b) U wrap. Figure 2(b) shows that a simple power equation gives a reasonable description of the relationship between the strength reduction factor and the axial rigidity of CFRP in beams which fail due to de-bonding of FRP. The majority of the data points lie above the curve when capacity reduction factors of 0.7 and 0.8 are applied to the lines of best fit in Figure 2(b) for side wrap and U wrap respectively. The resulting design equations for the effective strain ε_{fe} corresponding to de-bonding are given by

For side wrap

$$\varepsilon_{fe} = 0.7 \left\{ 40.25 \left(\rho_f E_f / f_c'^{(2/3)} \right)^{-0.70} \right\} \times 10^{-3} \leq 0.4\varepsilon_{fu} \leq 0.004 \quad (12a)$$

For U wrap

$$\varepsilon_{fe} = 0.8 \left\{ 29.14 \left(\rho_f E_f / f_c'^{(2/3)} \right)^{-0.48} \right\} \times 10^{-3} \leq 0.4\varepsilon_{fu} \leq 0.004 \quad (12b)$$

where ε_{fu} is the ultimate strain in FRP, ρ_f is the FRP shear reinforcement ratio, E_f is the elastic modulus of FRP (MPa) and f_c' is the compressive strength of the concrete (MPa). Equation 12 should be used with $z_f = 0.9d_f$ in Equation 2.

Equations 12a and 12b were used to calculate $V_{ftest}/V_{fproposed}$ for the specimens in Table 1. The resulting ratios $V_{ftest}/V_{fproposed}$ are plotted against the normalised axial rigidity of the CFRP in Figure 3. Comparison of Figures 1(a) to 1(c), Figure 3 and the statistics in Table 1 show that Equation 12 is more reliable than the other methods of which TR55 (Concrete Society, 2003) appears the best. Figure 4 compares the reduction factors R (with $\varepsilon_{fu} = 0.015$) given by Equation 12 with the corresponding values given by Khalifa *et al.* (1998) (Equation 4a), Triantafillou and Antonopoulos (2000) (Equation 7) and Zhang and Hsu (2005) (Equation 11). The method of Triantafillou and Antonopoulos (2000) has the disadvantage of not differentiating between side

Table 1. Comparison of measured and predicted V_f : (a) side wrap

Beam no.	f'_c : MPa	Section details		FRP properties and wrapping schemes					$V_{f_{test}}$: kN	$V_{f_{test}}/V_{f_{predicted}}$			
		b_w : mm	d : mm	d_f : mm	E_f : GPa	f_{fu} : MPa	t_f	$10^3 \rho_f$		Equation 12	Triantafillou	Khalifa	TR55
IB(C2)	60	152	267	267	235	3450	0.34	1.80	40.4	0.94	0.67	0.64	0.81
IB(C3)	60	152	267	267	235	3450	0.34	4.46	52.0	0.92	0.58	0.70	0.42
IB(C4)	60	152	267	152	235	3450	0.34	4.46	40.4	1.25	0.78	0.96	0.80
IB(C5) [§]	60	152	267	267	235	3450	0.34	1.80	60.6	—	0.98	0.69	0.88
IB(C6-45)	60	152	267	267	235	3450	0.34	1.80	69.3	1.14	0.81	0.77	0.98
IB(D6-45)	44	152	267	267	235	3450	0.34	1.80	70.9	1.34	0.93	0.97	1.15
A(a)	30	70	100	100	235	3055	—	2.20	13.4	2.33	1.52	—	—
A(b)	30	70	100	100	235	3055	—	2.20	11.1	1.94	1.26	—	—
A(c)	30	70	100	100	235	3055	—	2.20	10.7	1.88	1.22	—	—
A(45)	30	70	100	100	235	3055	—	2.20	13.8	1.71	1.11	—	—
AD(B4)	32	150	170	120	230	3400	0.17	2.23	19.4	1.29	0.85	5.67	1.11
AD(B5)	31	150	170	120	230	3400	0.17	2.23	21.1	1.42	0.93	6.23	1.22
AD(B6)	34	150	170	170	230	3400	0.17	2.23	41.6	1.90	1.25	1.74	1.25
C(RS90-1) ⁺	35	150	220	220	150	2400	1.00	6.67	34.3	0.97	0.58	0.55	0.93
C(RS90-2) ⁺	35	150	220	220	150	2400	1.00	6.67	41.8	1.18	0.71	0.67	1.13
C(RS135-1) ⁺	35	150	220	220	150	2400	1.00	4.44	40.8	0.92	0.59	0.69	1.17
C(RS135-2) ⁺	35	150	220	220	150	2400	1.00	4.44	46.3	1.05	0.67	0.78	1.33
CZ(T2)	56	260	500	500	238	2400	—	1.23	119.9	1.00	0.88	—	—
K(C-BT5)	35	150	355	255	228	3790	0.17	0.88	31.5	1.25	1.14	1.34	1.34
SA(S2)	45	200	260	260	230	3480	0.11	0.55	68.4	2.04	2.89	2.79	3.15
SA(S4)	38	200	260	260	230	3480	0.11	1.10	64.2	1.69	1.36	1.48	1.50
T(S1a)	30	70	100	100	235	3300	—	2.20	13.6	2.37	1.54	—	—
T(S1b)	30	70	100	100	235	3300	—	2.20	11.3	1.97	1.28	—	—
T(S2a)	30	70	100	100	235	3300	—	3.30	15.9	2.45	1.51	—	—
T(S2b)	30	70	100	100	235	3300	—	3.30	12.9	1.99	1.23	—	—
T(S3a)	30	70	100	100	235	3300	—	4.40	13.2	1.87	1.11	—	—
T(S3b)	30	70	100	100	235	3300	—	4.40	10.6	1.50	0.89	—	—
T(S1-45)	30	70	100	100	235	3300	—	2.20	14.1	1.74	1.13	—	—
T(S2-45)	30	70	100	100	235	3300	—	3.30	15.5	1.69	1.04	—	—
T(S3-45)	30	70	100	100	235	3300	—	4.40	12.2	1.22	0.72	—	—
TA (S2-45)	65	180	500	500	101	1450	—	6.67	200.6	1.24	0.84	—	—
TA (S3-45)	50	180	500	500	49	577	—	22.2	324.3	1.96	1.21	—	—
TA(S4-45)	49	180	460	460	71	708	—	8.80	212.1	1.68	1.11	—	—
TA(SR1-45)	54	180	460	460	71	708	—	4.40	177.9	1.65	1.36	—	—
TA(SR2-45)	53	180	460	460	71	708	—	8.80	244.9	1.86	1.24	—	—
Uj (5)	24	100	170	170	230	2650	0.10	1.94	20.1	1.68	1.09	4.42	0.96
Uj (6-45)	27	100	170	170	230	2650	0.10	1.94	24.0	1.34	0.88	3.45	0.80
Uj (7)	27	100	170	170	230	2650	0.19	3.90	32.3	2.07	1.24	1.34	0.92
Z(Z4 45)	42	152	200	200	165	2800	1.50	6.20	36.9	0.73	0.44	0.49	1.49
Z(Z4 90)	42	152	200	200	165	2800	1.50	6.20	27.6	0.77	0.47	0.52	1.57
Mean for side wrap										1.54	1.05	1.76	1.19
Standard deviation for side wrap										0.46	0.42	1.74	0.53

(continued)

and U-wrapped sections. Khalifa *et al.*'s (1998) Equation 4a gives an upper bound to R , which is frequently overridden by Equation 4b, which is based on bond failure. Equation 11 of Zhang and Hsu (2005) also gives an upper bound to R . Figure 4 shows that the relationship between the effective strain in the FRP and its axial rigidity is also evident in data from tests carried out by Khalifa and Nanni (2002) and the current authors in which the sheet thickness and the width of the beam were not varied. The authors consider there to be a genuine relationship between the axial rigidity

of CFRP and ϵ_{fe} which should be accounted for in design. Therefore, it is suggested that V_f is taken as the least of the values calculated with TR55 or Equation 2 with ϵ_{fe} from Equation 12 and $z_f = 0.9d_f$.

Experimental programme

Test specimens

Seven two-span, continuous RC beams with a rectangular cross-section of 152 mm by 305 mm and

Table 1. (continued)

Table 1. Comparison of measured and predicted V_f : (b) U wrap

Beam no.	f'_c : MPa	Section details		FRP properties and wrapping schemes					$V_{f_{test}}$: kN	$V_{f_{test}}/V_{f_{predicted}}$			
		b_w : mm	d : mm	d_f : mm	E_f : GPa	f_{fu} : MPa	t_f	$10^3 \rho_f$		Equation 12	Triantafillou	Khalifa	TR55
AD(B-7)	34	150	170	120	230	3400	0.17	2.23	29.3	0.99	1.24	1.10	1.07
AD(B-8)	35	150	170	170	230	3400	0.17	2.23	46.6	1.10	1.37	0.97	1.09
K(CW2)	28	150	255	255	228	3500	0.17	2.20	39.0	0.67	0.85	0.56	0.58
K(CO2)	21	150	255	255	228	3500	0.17	0.88	40.0	1.22	1.46	1.74	1.52
K(CO3)	21	150	255	255	228	3500	0.17	2.20	65.0	1.24	1.58	1.13	0.99
K(BT2)	35	150	355	255	228	3790	0.17	2.20	65.0	1.04	1.29	0.79	0.96
K(BT3)	35	150	355	255	228	3790	0.17	2.20	67.5	1.08	1.35	0.82	1.00
K(BT4)	35	150	355	255	228	3790	0.17	0.88	72.0	1.85	2.61	2.19	2.66
K(SW3-2)+	19	150	255	255	228	3790	0.17	2.20	50.5	0.98	1.26	0.92	0.77
K(SW4-2)+	19	150	255	255	228	3790	0.17	2.20	80.5	1.56	2.01	1.46	1.23
K(SO3-2)	28	150	255	255	228	3790	0.17	0.88	54.0	1.50	1.95	1.93	2.02
K(SO3-3)	28	150	255	255	228	3790	0.17	1.32	56.5	1.27	1.54	1.35	1.41
K(SO3-4)	28	150	255	255	228	3790	0.17	2.20	67.5	1.17	1.47	0.97	1.01
K(SO3-5)	28	150	255	255	228	3790	0.17	2.20	92.5	1.60	2.02	1.32	1.38
K(SO4-2)	28	150	255	255	228	3790	0.17	0.88	62.5	1.73	2.26	2.24	2.34
K(SO4-3)	28	150	255	255	228	3790	0.17	2.20	90.0	1.56	1.96	1.29	1.35
SA(S3)	41	200	260	260	230	3480	0.11	0.55	110.0	3.07	4.65	2.98	4.59
SA(S5)	40	200	260	260	230	3480	0.11	1.10	106.1	1.71	2.24	1.48	2.22
TK(BS2)	35	200	420	420	280	3494	—	0.17	39.2	2.18	2.73	—	—
TK(BS5)	37	200	420	420	280	3494	—	0.13	32.7	2.38	2.98	—	—
TK(BS6)	36	200	420	420	280	3494	—	0.09	30.0	3.23	4.03	—	—
Mean for U wrap										1.58	2.04	1.40	1.57
Std dev. for U wrap										0.67	0.94	0.62	0.95

§ Full wrap, + Includes steel stirrups, IB = Current paper, AD = Adhikary and Mutsuyoshi (2004), A = Antonopoulos (2000), AR = Araki *et al.* (1997), C = Chaallal *et al.* (1998), F = Funakawa *et al.* (1997), K = Khalifa *et al.* (1998), Khalifa and Nanni (2000, 2002), OM = Ono *et al.* (1997), SA = Sato *et al.* (1996), TK = Taerwe *et al.* (1997), T = Triantafillou (1998), Triantafillou and Antonopoulos (2000), TA = Taljsten (2003), Uj = Uji (1992), U = Umezu *et al.* (1997), Z = Zhang and Hsu (2005)

shear span-to-depth ratio (a/d) of 2.85 were tested. The effective depth to the steel reinforcement was 267 mm. Three 16 mm diameter bars were provided at the top and bottom of each beam. The yield strength of the reinforcement was 494 MPa. The corresponding flexural failure load of the beams is around 500 kN. No steel stirrups were provided within the interior shear spans. To ensure shear failure occurred within the central shear spans, 6 mm diameter steel stirrups were provided in the outer shear spans at 130 mm centres. Beam C1 was a control specimen so was not strengthened. The remaining tests investigated the contribution of different arrangements of CFRP to the shear capacity of the beams. The beams were not reinforced with internal stirrups within the central shear spans as the aim was to compare the efficiency of different arrangements of CFRP. Rectangular sections were tested since the aim was to compare the response of continuous beams with that of simply supported rectangular sections tested by others. One beam was fully wrapped and was tested as a limiting case to determine the influence of the CFRP anchorage length. Specimen C-4 was designed to simulate the reduced anchorage in an upstand beam. The CFRP

sheet was 0.34 mm thick. The elastic modulus of the carbon fibres was 234.5 GPa and the ultimate tensile strength was 3450 MPa. Details of the beams and reinforcement are shown in Figure 5.

Concrete mix

Beams C1 to C6 were cast from concrete mix 'A' which had a 28 day mean compressive cylinder strength of 60 MPa. Beam D6 was cast from concrete mix 'B' which had a 28 day mean compressive cylinder strength of 44 MPa. Both the mixes consisted of type I cement with maximum limestone coarse aggregate sizes of 19 mm and 13 mm for mixes 'A' and 'B' respectively.

Strengthening scheme

Figure 5 shows the configurations of CFRP used in the tests. The CFRP sheets were bonded to the vertical sides of the beams in all the beams except C5, which was fully wrapped. Prior to strengthening, the beam surfaces were cleaned of loose particles and form lines by grinding the concrete surface with an electric grinder. The edges of beam C5 were smoothed to reduce stress concentrations at these locations owing to the full wrapping of CFRP sheet. After surface preparation, the CFRP

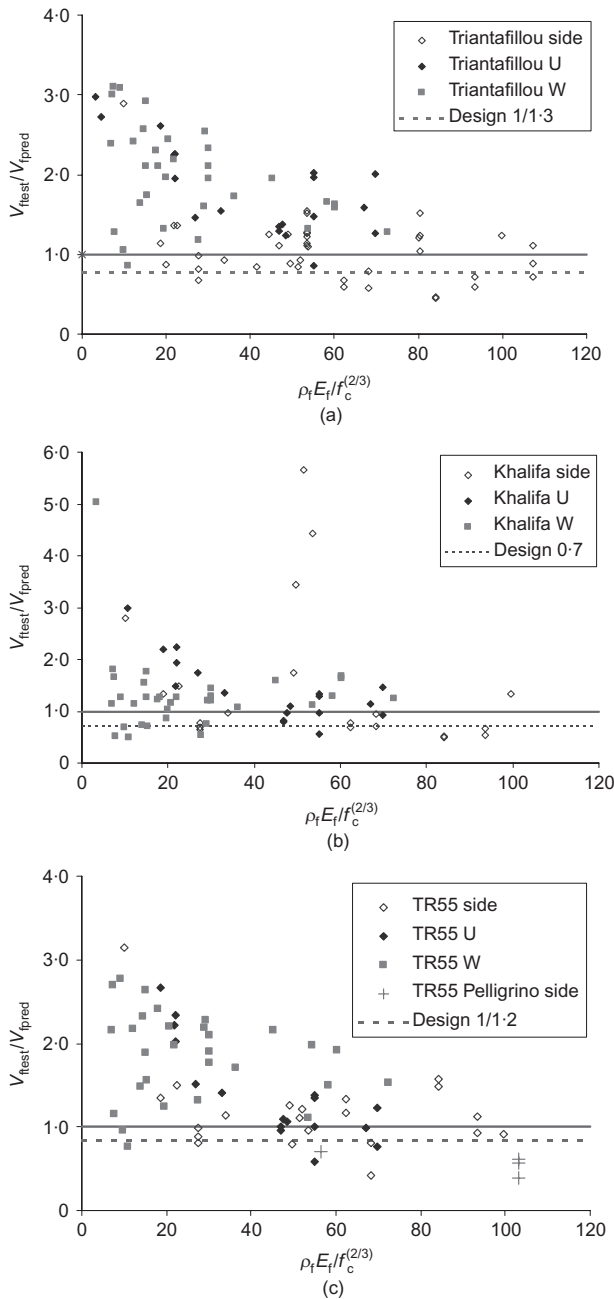


Figure 1. Comparison of measured and predicted V_f : (a) Triantafillou and Antonopoulos' method; (b) Khalifa et al.'s method; (c) TR55 method

sheet was cut to the required length and infused with two part epoxy. The surface was brushed and primed with one coat of epoxy. The saturated CFRP sheet was then applied to the sides of the beam at the required positions. In beams C2 to C5, the CFRP sheet was applied with the main fibres oriented perpendicular to the longitudinal axis of the beam. In beams C6 and D6, the direction of the main fibres was oriented at 45° to the longitudinal axis of the beam as shown in Figure 5.

Test set-up

Each beam was simply supported and continuous over two spans and loaded with a concentrated load at

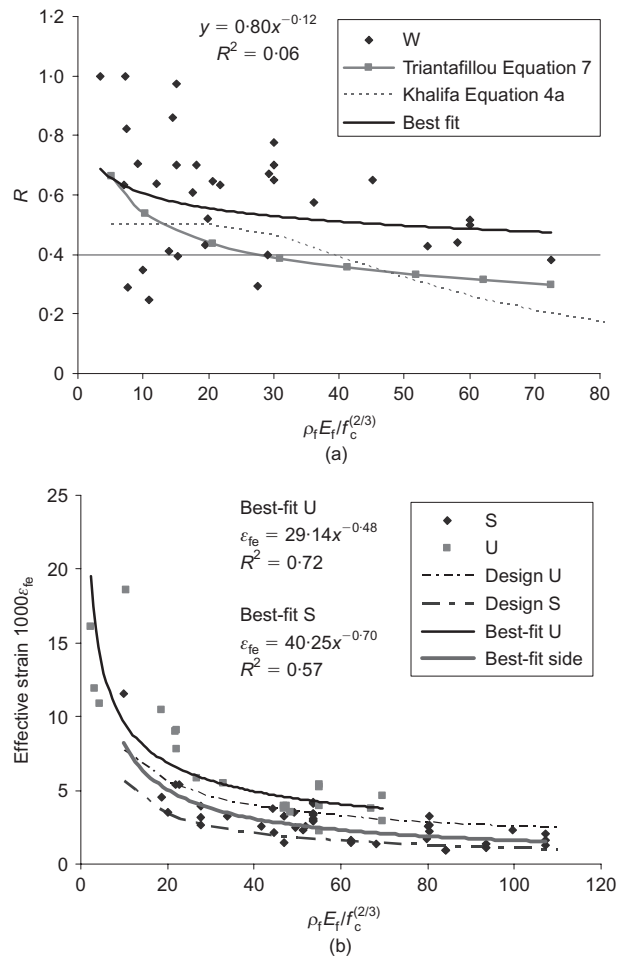


Figure 2. Proposed effective strain against normalised axial rigidity: (a) fracture of FRP; (b) de-bonding of FRP

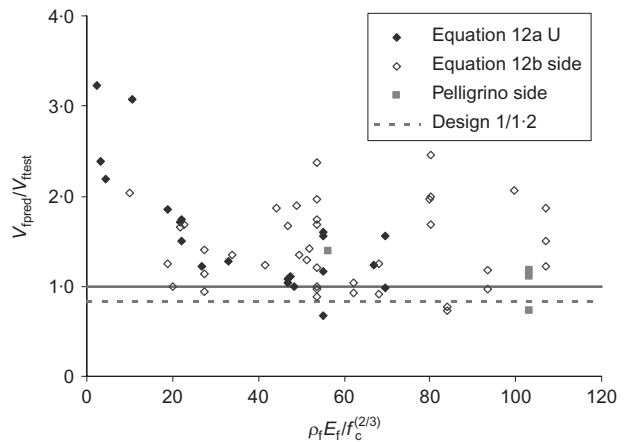


Figure 3. Comparison of measured and predicted V_f for Equation 12

the centre of each span, as shown in Figure 5. The load was applied with a 1000 kN capacity hydraulic jack. Linear variable displacement transducers (LVDTs) were used to measure vertical displacements at mid-span and over the supports. Strains were also

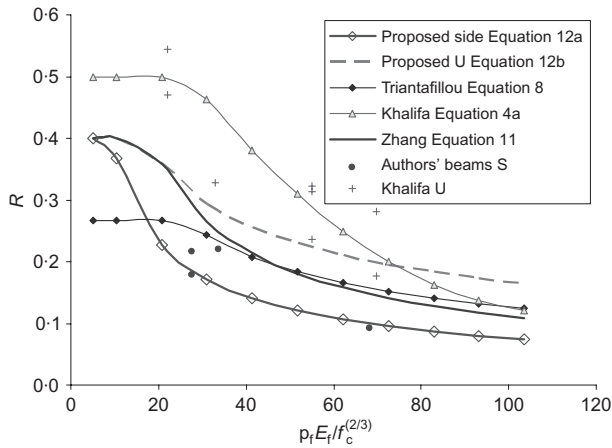


Figure 4. Comparison of strength reduction factors R ($\epsilon_{fu} = 0.015$)

measured in the CFRP on the vertical face of the beam with vertically oriented surface-mounted electrical resistance strain gauges. The strain gauges were located along the anticipated line of the diagonal shear crack at distances of 127, 330 and 533 mm from the face of the central support. The crack patterns at failure are shown in Figure 6.

Experimental results and discussion

The experimental results indicate that strengthening continuous RC beams in shear with CFRP sheet can be highly effective and that the contribution of the CFRP depends on its configuration and orientation. Of the seven beams tested, C1 was a control beam which was, consequently, not strengthened. Beam C1 failed at total load of 250 kN as a result of a shear-tension failure. The presence of CFRP sheets was found to alter the crack pattern from that observed in the control beam.

Beam C2 was strengthened with CFRP sheets measuring 304.8 mm by 304.8 mm, which were applied in the middle of each of the internal shear spans as shown in Figure 5. The beam failed in shear at total load of 384.7 kN, which is 54% greater than the control beam C1, owing to de-lamination of the CFRP sheet. Beam C5 was strengthened with a similar configuration of CFRP sheets to beam C2, but the sheets were fully wrapped rather than being side wrapped. A shear crack appeared at the mid-height of the beam near the central support at a load of 384.7 kN. The crack widened and travelled towards the internal support along the bottom face of the beam and upwards towards the load point. Clicking sounds were heard in the CFRP sheet when the load reached 403.9 kN, but the presence of the CFRP sheet stopped the crack from propagating and led to the formation of a second major diagonal crack between the load point and the CFRP sheet. The second

crack propagated along the tensile reinforcement towards the central support. De-lamination of the CFRP sheet was observed on both sides of the beam, but the beam failed as a result of CFRP sheet rupturing along with concrete splitting at the bottom face of the beam. The failure load of C5 was 452 kN which is 81% greater than the control beam C1 and 27% greater than beam C2. The deflection of the beam and the strain in the CFRP sheet were also greater than in beam C2.

Beam C3 was strengthened by complete side wrapping with CFRP sheets in the internal shear spans as shown in Figure 5. On loading, small flexural cracks appeared in the top face of beam above the central support. The cracks in the side faces of the beam were invisible during the test since they were obscured by the CFRP wrapping. Clicking sounds were heard as the load was increased and at 365.4 kN de-lamination occurred between the concrete and CFRP sheet under one of the load points. The beam failed at 423.2 kN, which is 69% greater than the control beam C1, due to de-lamination of the CFRP sheet. In addition, a longitudinal crack was also observed at the top face of the beam, which is indicative of a splitting failure. The CFRP sheet was removed after the test to see the cracking pattern at failure. The crack pattern was significantly different from the other beams in that the failure crack travelled along the bottom steel reinforcement, which is consistent with the arching action observed in the test. Loss of bond occurred between the steel reinforcement and concrete which resulted in separation of the concrete cover at the bottom face of the beam. Beam C4 was strengthened throughout the length of the shear span as in beam C3 but the CFRP sheets were only positioned within the tensile (i.e. upper) half of the beam depth as shown in Figure 5. The beam failed at 384.7 kN, which is 54% greater than the control beam C1, as a result of the concrete crushing and splitting along the bottom steel reinforcement and de-lamination of the CFRP sheet in the middle of the interior shear span.

In beam C6, 304.8 mm wide CFRP sheets were applied with the main fibres oriented almost perpendicular to the angle of the shear cracks at an angle of 45° to the longitudinal axis of the beam as shown in Figure 5. Beam C6 failed at a load of 480.9 kN, which is 92% greater than C1, as a result of the CFRP sheet de-laminating under the loading point. Yielding of the longitudinal reinforcement was observed at failure along with splitting of the concrete cover at the bottom face of the beam. The failure crack was inclined at a relatively steep angle of 58° to the longitudinal axis of the beam. Beam D6 was strengthened with the same configuration of CFRP sheet as beam C6 but the concrete compressive strength was 20% lower than in beam D6. Beam D6 failed at a total load of 461.7 kN, which is 7% less than C6, as a result of the CFRP sheet de-laminating from the beam surface.

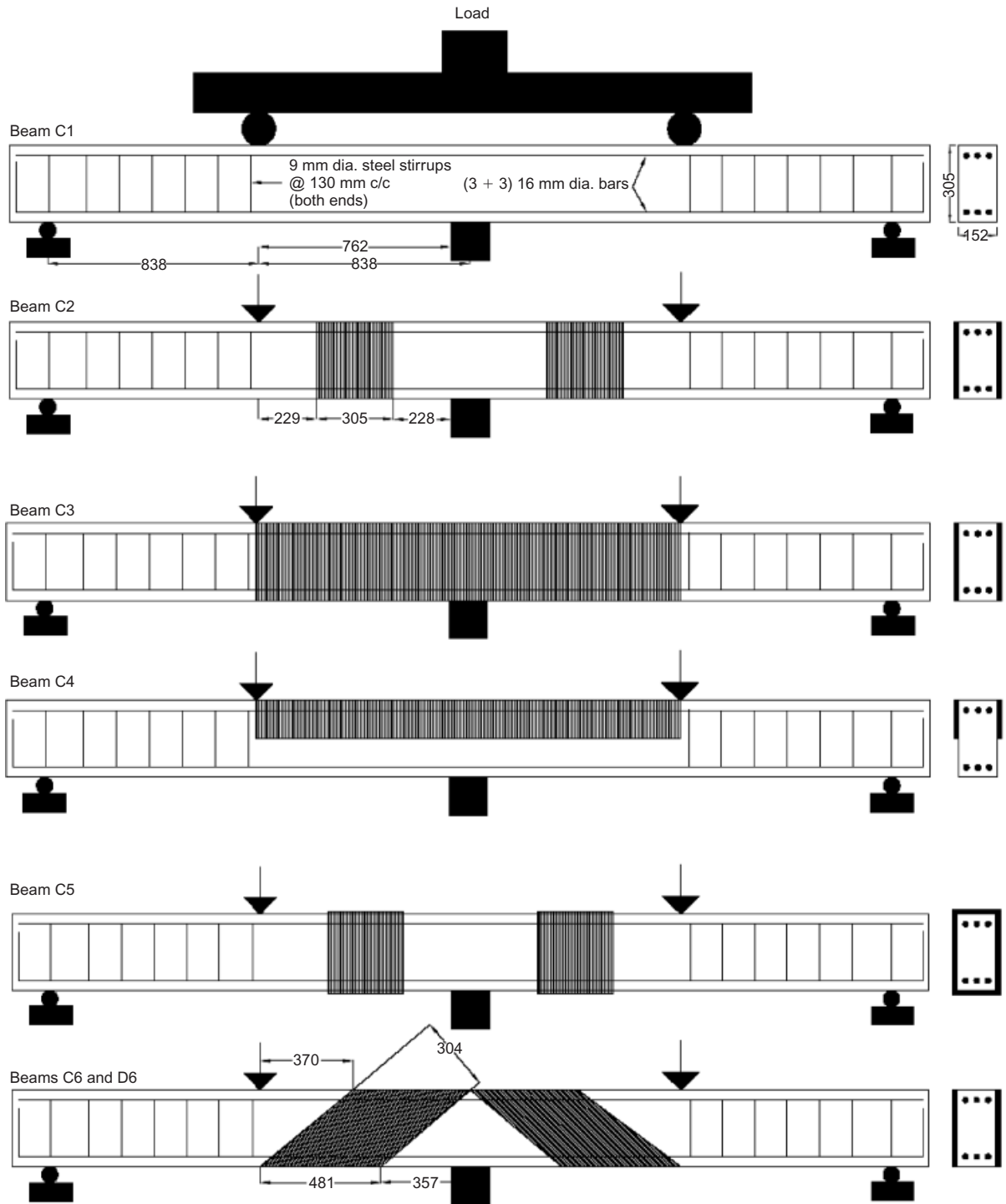


Figure 5. Beam configuration details

Shear strength

The shear strengths of the authors' beams are listed in Table 2. The tests showed that the surface area of the CFRP sheet can be minimised while maintaining a considerable increase in shear capacity. For example, the strength of beam C2 was only 15% less than that of beam C3 with complete side wrap even though the area of CFRP was reduced by 63% in beam C2. Placing the

CFRP over half the beam depth within the tensile zone as in Beam C4 (see Figure 5) increased shear strength but resulted in a brittle failure mode as shown in Figure 7 and is, therefore, not recommended. Applying CFRP within the central half of the shear span as in C2 (where the strength was increased by 54%) appears to be effective in continuous beams with ratios of shear span to effective depth up to at least 2.85. Tests C6 and D6 showed that shear strength is enhanced considerably

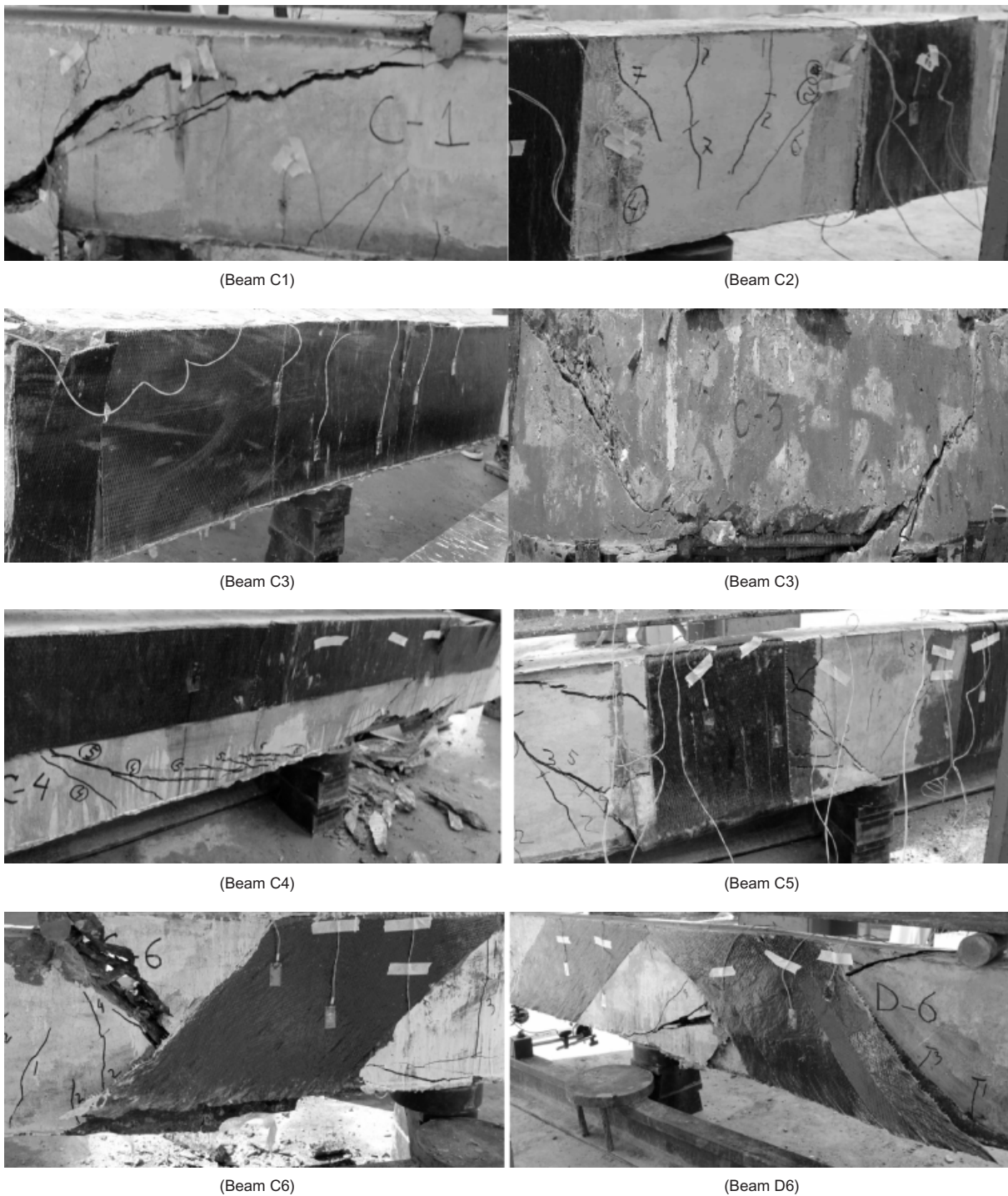


Figure 6. Crack pattern in tested beams

if the CFRP sheets are oriented with the main fibres at 45° .

Load–deflection behaviour

Figure 7 shows that all the CFRP strengthened beams were slightly stiffer and deflected more at the ultimate load than the control beam C1. The largest deflection occurred in beam C6 where the CFRP sheet was applied with the main fibres oriented at 45° to the long-
Magazine of Concrete Research, 2010, **62**, No. 1

itudinal axis of the beam. Beams C1, C2 and C4 showed brittle behaviour, whereas the other beams failed in a relatively ductile mode.

Load–strain behaviour

Figure 8 shows the variation in the vertical strains measured in the CFRP at the centre of the failed shear span. The strains were very small prior to diagonal cracking after which the strain increased rapidly. The

Table 2. Experimental results

	Ultimate load: kN	V_{exp} : kN	$V_{f,est}$: kN	Deflection: mm	$R_{strength}$	R_{strain}	Failure mode
C1	250	75.0	—	1.9	—	—	Shear
C2	384.7	115.4	40.4	2.68	0.18	0.08	Sheet delamination
C3	423.2	127.0	52.0	4.2	0.09	0.16	Sheet delamination
C4	384.7	115.4	40.4	3.9	0.12	0.18	Sheet delamination
C5	452.0	135.6	60.6	4.4	0.27	0.18	Sheet rupture
C6	480.9	144.3	69.3	5.3	0.22	0.32	Sheet delamination
D6	461.7	138.5	70.9	5.0	0.20	0.22	Sheet delamination

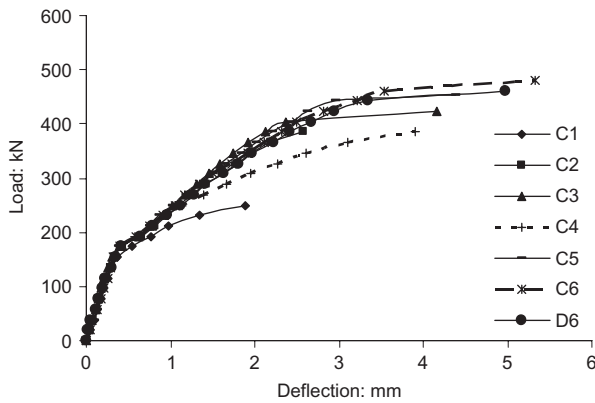


Figure 7. Load–mid-span deflection curves

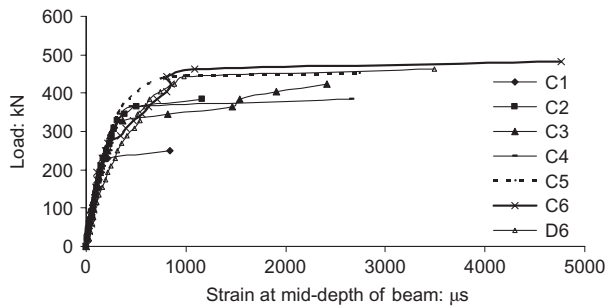


Figure 8. Load–vertical strain in CFRP sheet (mid-depth)

greatest strains were measured in beam C6 in which the CFRP sheet was applied at 45° to the longitudinal axis of the beam.

Analysis of current authors’ test beams

The contribution of the CFRP to shear strength was estimated for each beam by subtracting the shear strength of the control beam from that of the strengthened beams. The shear strength of the control beam was reduced by a factor of $(44/60)^{1/3}$ in the case of beam D6 to account for the difference in concrete strengths between beams C1 and D6. Two different methods were used to estimate the strength reduction factor R in Equation 3. First, reduction factors (R_{strain}) were obtained by dividing the peak strain measured in the FRP by its ultimate strain. Second, strength reduction factors ($R_{strength}$) were estimated from Equations 1 and 2. The resulting R values are given in Table 2. The

R values derived from the strains are of a similar order of magnitude to the values calculated from back substitution into Equations 1 and 2, but there is no consistent relationship between the two. The measured and predicted contributions of the CFRP to the shear strength are compared in Table 1, which shows that Equation 12 gives the best prediction of V_f . The FRP shear reinforcement ratio ρ_f was taken as $2t_f w_f / (b_w a_v)$ for the authors’ tests, which are designated with the prefix IB in Table 1, where t_f is the sheet thickness, w_f is the sheet width and a_v is the shear span of 762 mm. TR55 gives reasonable predictions of V_f for all the beams except C3 with complete side wrap where V_f is significantly overestimated.

Application of Eurocode 2

The ENV version of Eurocode 2 (British Standards Institution, 1992) included the ‘standard method’ for calculating the shear strength of beams which was equivalent to Equation 1. The ‘standard method’ was removed from Eurocode 2 (British Standards Institution, 2004) which only gives the variable strut inclination method for the design of shear reinforcement in beams. It is assumed in the variable strut inclination method that the shear force is entirely resisted by a truss consisting of concrete struts acting in compression equilibrated by shear reinforcement in tension. The angle of the concrete struts varies from 21.8 to 45° to the longitudinal axis of the beam depending upon the applied shear force. For members with inclined shear reinforcement, the design value of the shear strength is given by

$$V_{Rd,s} = A_{sw}(0.9d)f_{ywd}(\cot \theta + \cot \beta) \sin \beta / s \quad (13)$$

where A_{sw} is the area of steel shear reinforcement; f_{ywd} is the yield strength of the shear reinforcement; s is the spacing of the stirrups; θ is the angle in degrees of the concrete strut to the longitudinal axis of the beam; β is the inclination angle of shear reinforcement. The value of $\cot \theta$ is limited to $1 \leq \cot \theta \leq 2.5$. Eurocode 2²⁴ defines the maximum shear capacity in terms of $\cot \theta$ and the effective crushing strength of the concrete as follows for beams with vertical stirrups

$$V_{Rd,max} = 0.9b_w d \nu f_{cd} / (\cot \theta + \tan \theta) \quad (14)$$

where ν is a strength reduction factor for concrete with skew cracks and f_{cd} is the design concrete strength.

The variable angle truss model is an idealisation based on the lower bound theorem of plasticity in which all the shear force is assumed to be resisted by the stirrups. In reality, the angle of the compression field in the truss is steeper than assumed in Eurocode 2 and part of the shear force is resisted by V_c , which is not constant as assumed in Equation 1. The following issues are relevant to the application of the variable angle truss model to beams strengthened in shear with CFRP.

- (a) Figure 9 shows that Eurocode 2 (British Standards Institution, 2004) gives greater shear strengths than Equation 1 if the reinforcement index exceeds a critical value of around twice the minimum value specified in Eurocode 2.
- (b) The area of steel shear reinforcement contributing to the shear strength is assumed to be constant in the ‘standard method’ but varies with $\cot\theta$ in Equation 13. The contribution of steel shear reinforcement to shear strength is reduced when the beam is strengthened with FRP if the design shear force is sufficiently high to govern the maximum permissible value of $\cot\theta$.
- (c) Tests show that internal steel stirrups and external CFRP shear reinforcement are most efficient when oriented at 45° . This can be seen by comparing the shear strengths of the authors’ beams C2, C5, C6 and D6 or Chaallal *et al.*’s (1998) beams RS90 and RS135. The increased efficiency of inclined stirrups is not reflected in Equation 13 which predicts that changing the orientation of the shear reinforcement FRP from 90° to 45° reduces the shear strength by 1% if $\cot\theta=2.5$.
- (d) The procedure of deriving the effective stress ($E\varepsilon_{fe}$) in CFRP from test data with Equations 1 and 2 is dubious since V_c is not constant as assumed and the truss angle is not 45° . The procedure would give very different stresses to the yield stress if used for beams with steel stirrups.

Equation 13 can be modified as follows to give the shear strength of beams without internal stirrups strengthened with CFRP

$$V_{Rd,FRP} = Cz_f b_w E_f (\cot\theta + \cot\beta) \sin\beta \quad (15)$$

where C is the least of either $\rho\varepsilon_{fe}$ Equation 12 or $\rho^*\varepsilon_{fe}$ TR55 where ρ is the FRP ratio defined below Equation 2, ρ^* is defined in Equation 9 and ε_{fe} is calculated in accordance using Equation 12 or TR55 (Concrete Society, 2003) as noted. The following methods were investigated for calculating the shear strength ($V = V_c + V_s + V_f$) of beams strengthened with CFRP with Eurocode 2.

- (a) Method 1: $V_c + V_s$ was taken as the greatest of V_c or $V_{Rd,s}$ from Equation 13 with the maximum permissible value of $\cot\theta$ corresponding to the shear capacity of the strengthened beam. V_f was calculated using Equation 15 with $\cot\theta = 1$.

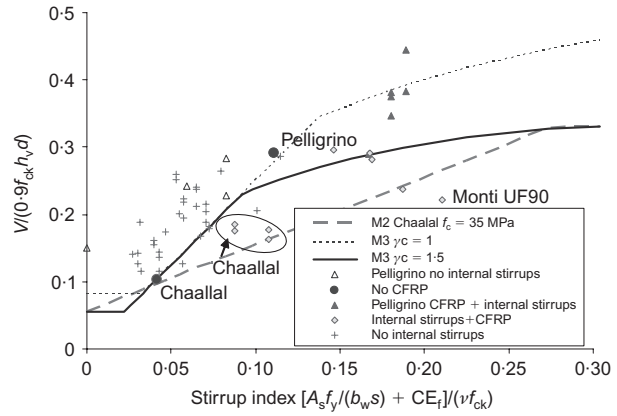
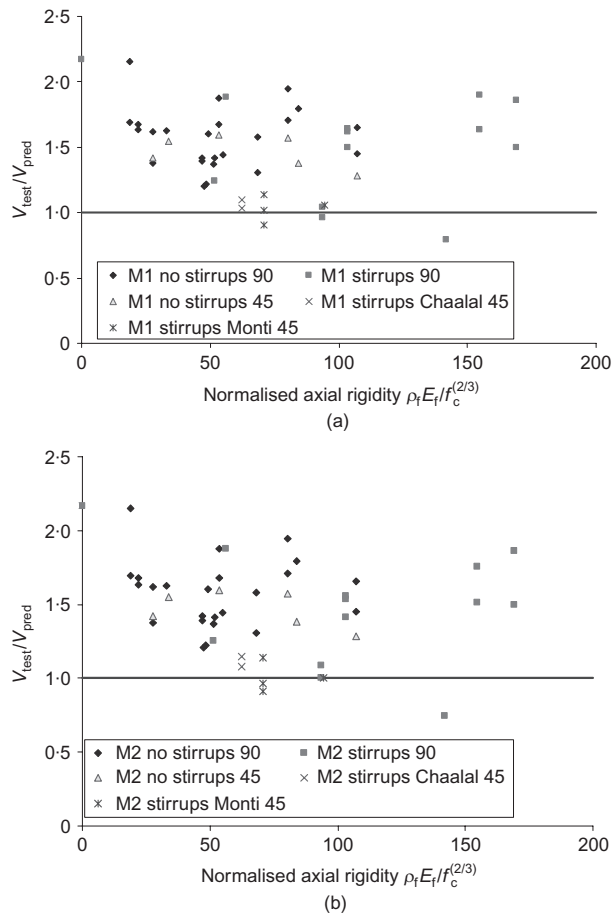


Figure 9. Comparison between measured and predicted shear strengths

- (b) Method 2: $V_c + V_s$ was taken as $V_c + V_{Rd,s}$ where $V_{Rd,s}$ was calculated using Equation 13 with $\cot\theta = 1$. V_f was calculated as in (a) above.
- (c) Method 3: As (a) above but V_f was calculated with Equation 15 using the value of $\cot\theta$ used for $V_{Rd,s}$ in Equation 13. $V = V_c + V_s + V_f$ was not taken as less than V_c .

The methods were assessed for beams within the authors’ database with U or side wrapping where sufficient data were available. The database consisted of 30 beams reinforced in shear with only CFRP (six beams from this study, five beams from Adhikary and Mut-suyoshi (2004) (B-4 to B-8 inclusive), eight beams from Khalifa and Nanni (2002, 2000) (BT2 to BT5 inclusive and SO3-2 to SO3-4 and SO4-2), nine beams from Triantafillou (1998) (S1a, S1b, S2a, S2b, S3a, S3b, S1-45 to S3-45) and two beams from Zhang and Hsu (2005) (Z4 45, Z4 90)) and 20 beams with CFRP and steel shear reinforcement (four beams from Chaallal *et al.* (1998), all 11 beams from Pelligrino and Modena (2002) and five beams from Monti and Liotta (2007) (UF90, UF45+A, UF45+D, WS45+, UF90)). The beams of Monti and Liotta (2007) and Pelligrino and Modena (2002) are not included in Table 1. The CFRP was oriented at 90° in all the beams except those with 45 in their label where the orientation was 45° . The beams of Monti and Liotta (2007) had unusually low concrete cube strengths of 13.3 MPa. The top of the CFRP was stopped 150 mm below the top of these beams, which had an effective depth of 410 mm, to simulate the presence of a flange. The top of the sheet was mechanically anchored in all the beams except UF90, which had a comparatively low strength.

The strengths of the beams are compared in Figure 9 with the strengths calculated with method 3. Figure 9 shows that method 3 overestimates the strength of a significant number of beams with stirrups and is therefore not recommended. Method 2 is illustrated in Figure 9 (with $\gamma_c = 1.5$ and $\beta = 90^\circ$) for Chaalal *et al.*’s beams in which f'_c was 35 MPa. Figures 10(a) and 10(b), in which the material factors of safety were



Figures 10. Comparison between measured and predicted shear strengths ($\gamma_c = 1.5$): (a) method 1 ($V_f = \text{minimum from TR55 or Equation 12}$); (b) method 2 ($V_f = \text{minimum from TR55 or Equation 12}$)

taken as 1.5 for concrete and 1.0 for steel and CFRP, show that methods 1 and 2 give similar results for the beams in the database. Figures 9 and 10 show all three methods are less conservative for beams with internal steel shear reinforcement, which suggests that the principle of superposition assumed in Equation 1 is not strictly valid due to strain incompatibility. The reduced efficiency of CFRP in beams with internal stirrups is related to two fundamental issues. First, the presence of internal stirrups changes the crack pattern. A single dominant shear crack tends to form in beams without internal stirrups strengthened with CFRP whereas multiple parallel shear cracks form in beams with internal stirrups. The influence of stirrups on the crack pattern, and consequently the anchorage of the CFRP, which determines its effective area, is not included in the design methods discussed in this paper or that of Monti and Liotta (2007).

Second, methods 1 to 3 which utilise the lower bound theorem of plasticity, assume

- (a) that the internal stirrups yield at failure; and
- (b) that the effective strain in the CFRP at failure is

independent of the area of internal shear reinforcement.

Assumption (a) is only credible if the strain in the CFRP at failure is sufficient for the internal stirrups to yield. Strain measurements such as those in Figure 8 suggest this is likely to be the case unless the axial rigidity of the CFRP is very high. In methods 1 to 3, Equation 13 is used to calculate $V_c + V_s$ (with $\cot\theta$ calculated in terms of the shear capacity of the strengthened beam) whereas in method 2, $V_c + V_s$ is taken as the design shear strength of the un-strengthened beam. Providing the stirrups yield, both approaches imply $V_c + V_s$ is independent of the strain in the stirrups, which is not generally the case since shear failure is relatively brittle. In reality, loss of aggregate interlock is likely to reduce $V_c + V_s$ if the crack widths in the strengthened beam are greater than in the un-strengthened beam at failure. $V_c + V_s$ is also likely to reduce if the strain in the internal stirrups at failure is less in the strengthened than un-strengthened beam. Figure 9 shows that the variable angle truss model in Eurocode 2 can give significantly higher shear strengths than the ‘standard method’ for beams with internal steel stirrups. It follows that method 1 can give significantly higher strengths for strengthened beams with CFRP than method 2 which calculates $V_s + V_c$ using the ‘standard method’. The current authors consider it unwise to take advantage of this increase in strength for reasons discussed above. Therefore, it is suggested in the absence of further test data to the contrary that method 2 is used to assess the shear strength of beams strengthened with CFRP.

Conclusions

This paper describes a series of six tests on continuous beams strengthened in shear with CFRP. The tests showed that it is beneficial to orientate the fibres in the CFRP sheets at 45° so that they are approximately perpendicular to the shear cracks. The tests also support the hypothesis that the efficiency of CFRP reduces with its axial rigidity. TR55 (Concrete Society, 2003) is unique among the design methods considered in this paper in not relating the effective strain in CFRP to its axial rigidity. Consequently, TR55 (see Figure 1(c)) was found significantly to overestimate V_f in some beams including ones tested by the current authors and Pelligrino and Modena (2002). Therefore, it is suggested that TR55 should be modified to include Equations 12a and 12b, which relate the effective strain in CFRP to its axial rigidity in side and U-wrapped sections respectively.

It is shown that the variable angle truss model in Eurocode 2 can overestimate the shear strength of beams with internal stirrups that are strengthened with CFRP. This implies CFRP strengthened beams can have

insufficient ductility for the lower bound theorem of plasticity to be valid. Therefore, it is recommended that shear strength is calculated by adding the individual contributions calculated for the concrete V_c , internal steel stirrups V_s , and CFRP V_f with V_s and V_f calculated with a 45° truss because this reduces the ductility demand on the beam.

References

- ACI (American Concrete Institute) (2002) *Guide for the Design and Construction of Externally Bonded FRP Systems for Strengthening Concrete Structures*. ACI, Farmington Hills, Michigan, USA, 2002. ACI Committee 440.
- Adhikary BB and Mutsuyoshi H (2004) Behavior of concrete beams strengthened in shear with carbon-fiber sheets. *Journal of Composites for Construction* **8**(3): 258–264.
- Antonopoulos CP (2000) *Shear Strengthening of Reinforced Concrete Structures using Composite Materials*. Diploma thesis, Department of Civil Engineering, University of Patras, Greece.
- Araki N, Matsuzaki Y, Nakano K, Kataoka T and Fukuyama H (1997) Shear capacity of retrofitted RC members with continuous fiber sheets. *Proceedings of the Third Symposium on Non-Metallic (FRP) Reinforcement for Concrete Structures, Japan* **1**: 515–522.
- British Standards Institution (1992) *ENV 1992-1, Eurocode2: Design of Concrete Structures: General Rules for Buildings*. BSI, London, 1992.
- British Standards Institution (2004) *Eurocode 2-1: Design of Concrete Structures: General Rules for Buildings*. BSI, London, 2004.
- Chaallal O, Nollel MJ and Perraton D (1998) Shear strengthening of RC beams by externally bonded side CFRP strips. *Journal of Composites for Construction* **2**(2): 111–113.
- Concrete Society (2003) *Design Guidance for Strengthening Concrete Structures Using Fibre Composite Materials*. Concrete Society, Camberley, 2003. Technical Report 55.
- Denton SR, Shave JD and Porter AD (2004) Shear strengthening of reinforced concrete structures using FRP composites. In *Advanced Polymer Composites for Structural Applications in Construction* (Holloway LC, Chrssanthopoulos MK and Moy SSJ (eds)). Woodhead Publishing, Cambridge, pp. 134–143.
- Funakawa I, Shimono K, Watanbe T, Asada S and Ushijima S (1997) Experimental study on shear strengthening with continuous fiber reinforcement sheet and methyl methacrylate resin. *Non-Metallic (FRP) Reinforcement for Concrete Structures*. Japan Concrete Institute, Tokyo, Vol. 1, pp. 475–482.
- Horiguchi T and Saeki N (1997) Effect of test methods and quality of concrete on bond strength of CFRP sheet. *Proceedings of the Third Symposium on Non-Metallic (FRP) Reinforcement for Concrete Structures, Japan* **1**: 265–270.
- International Federation for Concrete (fib) (2001) *Externally Bonded FRP Reinforcement for RC Structures*. The International Federation for Concrete, Lausanne, 2001.
- Khalifa A and Nanni A (2000) Improving shear capacity of existing RC T-section beams using CFRP composites. *Cement and Concrete Composites* **22**(2): 165–174.
- Khalifa A and Nanni A (2002) Rehabilitation of rectangular simply supported RC beams with shear deficiencies using CFRP composites. *Construction and Building Materials* **16**(3): 135–146.
- Khalifa A, Gold W, Nanni A and Abdel-Aziz MI (1998) Contribution of externally bonded FRP to the shear capacity of RC flexural members. *Journal of Composites for Construction* **2**(4): 195–202.
- Monti G and Liotta M (2007) Tests and design equations for FRP strengthening in shear. *Construction and Building Materials* **21**(4): 799–809.
- Ono K, Matsumura M, Sakanishi S and Miyata K (1997) Strength Improvement of RC bridge piers by carbon fiber sheet. In *Non-Metallic (FRP) Reinforcement for Concrete Structures*. Japan Concrete Institute, Tokyo, Vol. 1, pp. 563–570.
- Pelligrino C and Modena C (2002) Fiber reinforced polymer shear strengthening of reinforced concrete beams with transverse reinforcement. *Journal of Composites for Construction* **6**(21): May, 104–111.
- Sato Y, Ueda T, Kakuta Y and Tanaka T (1996) Shear reinforcing effect of carbon fiber sheet attached to side of reinforced concrete beams. *Advanced Composite Materials in Bridges and Structures* (El-Badry MM (ed.)), CSCE, Montreal, Canada, pp. 621–627.
- Taerwe L, Khalil H and Matthys S (1997) Behaviour of RC beams strengthened in shear by external CFRP sheets. In *Non-Metallic (FRP) Reinforcement for Concrete Structures*. Japan Concrete Institute, Tokyo, Vol. 1, pp. 483–490.
- Triantafillou TC (1998) Shear strengthening of reinforced concrete beams using epoxy-bonded FRP composites. *ACI Structural Journal* **95**(2): Mar.–Apr., 107–115.
- Triantafillou TC and Antonopoulos CP (2000) Design of concrete flexural members strengthened in shear with FRP. *Journal of Composites for Construction* **4**(4): 198–205.
- Taljusten B (2003) Strengthening concrete beams for shear with CFRP sheets. *Construction and Building Materials* **17**(1): 15–26.
- Uji K (1992) Improving shear capacity of existing reinforced concrete members by applying carbon fiber sheets. *Transactions of the Japan Concrete Institute* **14**: 253–266.
- Umezu K, Fujita M, Nakai H and Tamaki K (1997) Shear behaviour of RC beams with aramid fiber sheet. *Proceedings of the Third Symposium on Non-Metallic (FRP) Reinforcement for Concrete Structures, Japan*, 491–498.
- Zhang Z and Hsu T (2005) Shear strengthening of reinforced concrete beams using carbon-fiber-reinforced polymer laminates. *Journal of Composites for Construction* **9**(2): 158–169.

Discussion contributions on this paper should reach the editor by 1 July 2010